Automatica 179 (2025) 112433

Contents lists available at ScienceDirect

Automatica

journal homepage: www.elsevier.com/locate/automatica

Brief Paper

Output feedback periodic event-triggered and self-triggered boundary control of coupled 2×2 linear hyperbolic PDEs ☆

Eranda Somathilake [a,*], Bhathiya Rathnayake [b], Mamadou Diagne [a]

[a] Department of Mechanical and Aerospace Engineering, University of California, San Diego, La Jolla, CA 92093, USA
[b] Department of Electrical and Computer Engineering, University of California, San Diego, La Jolla, CA 92093, USA

ARTICLE INFO

Article history:
Received 3 June 2024
Received in revised form 12 May 2025
Accepted 17 May 2025

Keywords:
Backstepping control design
Coupled hyperbolic systems
Observer design
Periodic event-triggered control
Self-triggered control
Saint-Venant model

ABSTRACT

In this paper, we expand recently introduced observer-based periodic event-triggered control (PETC) and self-triggered control (STC) schemes for reaction–diffusion PDEs to boundary control of 2×2 coupled hyperbolic PDEs in canonical form and with anti-collocated measurement and actuation processes. The class of problem under study governs transport phenomena arising in water management systems, oil drilling, and traffic flow, to name a few. Relative to the state of the art of observer-based event-triggered control of hyperbolic PDEs, our contribution goes two steps further by proposing observer-based PETC and STC for the considered class of systems. These designs arise from a non-trivial redesign of an existing continuous-time event-triggered control (CETC) scheme. PETC and STC eliminate the need for constant monitoring of an event-triggering function as in CETC; PETC requires only periodic evaluations of the triggering function for event detection, whereas STC is a "predictor-feedback" that anticipates the next event time at the current event exploiting continuously accessible output measurements. The introduced resource-aware designs act as input holding mechanisms allowing for the update of the input signal only at events. Subject to the designed boundary output feedback PETC and STC control laws characterized by a set of event-trigger design parameters, the resulting closed-loop systems, which are inherently Zeno-free by design, achieve exponential convergence to zero in the spatial L^2 norm. We illustrate the feasibility of the approach by applying the control laws to the linearized Saint-Venant model, which describes the dynamics of shallow water waves in a canal and is used to design flow stabilizers via gate actuation. The provided simulation results illustrate the proposed theory.

© 2025 Elsevier Ltd. All rights are reserved, including those for text and data mining, AI training, and similar technologies.

1. Introduction

Hyperbolic PDEs are useful for the estimation, prediction, and control of various systems such as open channel fluid flow (Bastin & Coron, 2011; Coron, d'Andréa Novel, & Bastin, 1999; Diagne, Diagne, Tang & Krstic, 2017; Diagne, Tang, Diagne & Krstic, 2017; Halleux, Prieur, Coron, dÄndréa Novel, & Bastin, 2003), water–sediment dynamic systems (Diagne, Diagne, et al., 2017; Diagne, Tang, et al., 2017; Somathilake & Diagne, 2024) and traffic systems (Burkhardt, Yu, & Krstic, 2021; Yu & Krstic, 2022). Output-feedback control of 2×2 hyperbolic PDEs is presented in Vazquez, Krstic, and Coron (2011) via the backstepping approach with further developments in Di Meglio, Vazquez, and Krstic (2013), Hu, Di Meglio, Vazquez, and Krstic (2016). Subsequent advancements led to the design of adaptive observers in Anfinsen, Diagne, Aamo, and Krstic (2016, 2017) and adaptive boundary control strategies in Anfinsen and Aamo (2019). In the contributions reported above, global exponential stability is principally established with respect to the L^2 norm of the state, and both full-state feedback and observer-based control design are considered.

1.1. Event-based control of linear coupled hyperbolic systems

The aforementioned results on the boundary control hyperbolic PDEs rely on continuous-time control (CTC), which is often not feasible. A practical solution is sampled-data control, where the control input is updated according to a predetermined sampling schedule. However, the maximum allowable sampling interval of this schedule must be chosen conservatively to ensure that the control input is updated frequently. Alternatively,

☆ This work was funded by the USA National Science Foundation CAREER Award CMMI-2302030 and the USA National Science Foundation grant CMMI-2222250. The material in this paper was partially presented at the 2025 American Control Conference, (ACC), July 8–July 10, 2025, Denver, Colorado, USA. An extended version of the paper can be found at Somathilake et al. (2024). This paper was recommended for publication in revised form by Associate Editor Yang Zhu under the direction of Editor Miroslav Krstic.

* Corresponding author.
E-mail addresses: esomathilake@ucsd.edu (E. Somathilake), brm222@ucsd.edu (B. Rathnayake), mdiagne@ucsd.edu (M. Diagne).

https://doi.org/10.1016/j.automatica.2025.112433
0005-1098/© 2025 Elsevier Ltd. All rights are reserved, including those for text and data mining, AI training, and similar technologies.

event-triggered control (ETC) introduces feedback into the control update tasks. Here, the control input is updated only when a certain condition related to the system states is met, which we call an *event*. This feedback integration means the schedule of control update times is not restricted by a worst-case scenario. Control updates are triggered based on the current state rather than an unlikely worst-case scenario, leading to significantly sparser control updates compared to traditional sampled-data control methods.

The latest advancements in control systems theory have witnessed an unprecedented expansion in event-based control applied to PDE systems. ETC for parabolic PDEs involving both static and dynamic triggering conditions can be found in Espitia, Karafyllis, and Krstic (2021), Rathnayake and Diagne (2024a), Rathnayake, Diagne, Espitia, and Karafyllis (2021), Rathnayake, Diagne, and Karafyllis (2022), Wang and Krstic (2022a). Dealing with event-based boundary control of hyperbolic systems, our current contributions align with works such as Espitia (2020), Wang and Krstic (2022b) with particular emphasis on Espitia (2020), which proposes a globally exponentially convergent observer-based ETC for a 2×2 hyperbolic system in the canonical form. The authors of Diagne and Karafyllis (2021) design a static triggering condition that achieves exponential stabilization of a scalar but nonlinear hyperbolic system describing parts flow in a highly re-entrant manufacturing plant. The model of concern is often used to describe semi-conductors and chip assembly lines.

1.2. Contributions

This contribution presents two major improvements relative to the state of the art of observer-based ETC for hyperbolic PDEs by removing the necessity of continuous monitoring of the triggering functions, an unavoidable step when implementing the regular ETC stabilizer (for instance Espitia, 2020), which we refer to as *continuous-time* ETC (CETC). This enables the controller to be implemented in a digital platform. The *periodic* ETC (PETC) mechanism proposes a method in which the triggering function is periodically evaluated to determine if the input needs to be updated. In contrast, sampled-time control updates the control input at fixed time intervals. The *self-triggered control* (STC) determines the next triggering time during the current triggering instance.

The PETC and STC designs introduced for a scalar reaction–diffusion PDE with explicit gain kernel functions (Rathnayake & Diagne, 2024b) are proven to apply to hyperbolic PDE systems of a higher level of complexity induced by coupled dynamics, leading to implicitly defined coupled gain kernel functions. The authors of Zhang, Rathnayake, Diagne, and Krstic (2025) proposed *full-state feedback* PETC and STC designs for a 2×2 coupled hyperbolic traffic PDEs exploring the notion of a *performance barrier* (Ong & Cortés, 2023; Rathnayake, Diagne, Cortés, & Krstic, 2025). However, *observer-based* PETC and STC designs for hyperbolic PDEs are still lacking, despite being crucial for practical control implementations in the context of flow and fluid systems for which distributed measurements of the state is often implausible. To address this significant gap, this work presents observer-based PETC and STC designs for 2×2 coupled hyperbolic PDEs applied to the linearized Saint-Venant equations modeling water flow and level regulation problem via gate actuation.

Both PETC and STC are inherently free from Zeno behavior, and the well-posedness of the closed-loop system under both PETC and STC is provided. Furthermore, using Lyapunov arguments, we establish the exponential convergence of the closed-loop signals to zero in the L^2 spatial norm. The rapid development of remote actuation systems for automated control of networks of irrigation canals justifies the application example as preserving actuation and communication resources. This enables the expansion of the level of autonomy by drastically reducing energy and bandwidth consumption while also providing methods that can be implemented on digital infrastructure. In addition, elimination of the continuous movement of the sluice gate will reduce the deterioration of the gate actuation mechanism with time.

Organization of the paper: Section 2 presents an exponentially stabilizing boundary control law for a 2×2 linear hyperbolic system followed by its emulation for the event-triggering mechanisms as well as necessary preliminary results for the proposed control designs including the CETC design. Sections 3 and 4 present the exponentially convergent PETC, and STC event-triggering mechanisms. Finally, we present the numerical simulations of the control strategies applied to the linearized Saint-Venant equations and concluding remarks in Sections 5 and 6, respectively.

Notation. Let $\mathbb{R}$ be the set of real numbers and $\mathbb{R}^+$ be the set of positive real numbers. Let $\mathbb{N}$ be the set of natural numbers including 0. Define the constant $\ell \in \mathbb{R}^+$. By $L^2(0,\ell)$, we denote the equivalence class of Lebesgue measurable functions $f : [0,\ell] \to \mathbb{R}$ such that $\|f\|_{L^2((0,\ell);\mathbb{R})} = \left(\int_0^\ell |f(x)|^2\right)^{1/2} < \infty$. Define $\mathcal{C}^0(I; L^2((0,\ell);\mathbb{R}))$ as the space of continuous functions $u(\cdot,t)$ for an interval $I \subseteq \mathbb{R}^+$ such that $I \ni t \to u(\cdot,t) \in L^2((0,\ell);\mathbb{R})$. Also, for the equivalence class of Lebesgue measurable functions $\chi_1, \chi_2 : [0,\ell] \to \mathbb{R}$, we define $\|(\chi_1,\chi_2)^T\| = \left(\|\chi_1\|^2_{L^2((0,\ell);\mathbb{R})} + \|\chi_2\|^2_{L^2((0,\ell);\mathbb{R})}\right)^{1/2}$.

2. Preliminaries and problem formulation

We consider the following 2×2 linear hyperbolic PDE system in the canonical form where the independent variables $t \geq 0$ and $x \in [0,\ell]$ are time and space variables, respectively, and the PDE states $u(x,t)$ and $v(x,t)$ satisfy

$$\partial_t u(x,t) = -\lambda_1 \partial_x u(x,t) + c_1(x) v(x,t), \quad (1)$$

$$\partial_t v(x,t) = \lambda_2 \partial_x v(x,t) + c_2(x) u(x,t), \quad (2)$$

with boundary conditions

$$u(0,t) = q v(0,t), \quad v(\ell,t) = \rho u(\ell,t) + U(t). \quad (3)$$

Here, $U(t)$ is the continuous-time boundary control input, and $\lambda_1, \lambda_2 \in \mathbb{R}^+$, $c_1(x), c_2(x) \in \mathcal{C}^0((0,\ell);\mathbb{R})$. Further, $q \neq 0$ is the distal reflection term, and $\rho \neq 0$ is the proximal reflection term. The initial conditions are such that $(u^0,\ v^0)^T \in L^2((0,\ell);\mathbb{R}^2)$. We make the following assumption on the reflection terms.

Assumption 1 (*Espitia, 2020*)**.** The reflection terms are small enough such that $|\rho q| \leq \frac{1}{2}$.

2.1. Continuous-time output feedback control and its emulation for ETC

In this subsection, we develop a continuous-time backstepping output feedback control $U(t)$ capable of exponentially stabilizing the closed-loop system consisting of the plant (1)–(3) and an observer, using $v(0,t)$ as the available boundary measurement. Since the actuation and measurement are located at opposite boundaries, this setup is referred to as anti-collocated sensing and actuation, which differs from the configuration in Espitia (2020), where both the actuation and measurement are located at the same boundary.

We design an observer consisting of the copy of the plant plus some output injection terms with the observer states denoted by

$(\hat{u}, \hat{v})^T$. Defining the observer errors as $\tilde{u} := u - \hat{u}$, $\quad \tilde{v} := v - \hat{v}$, the following observer is proposed:

$$\partial_t \hat{u}(x,t) = -\lambda_1 \partial_x \hat{u}(x,t) + c_1(x)\hat{v}(x,t) + p_1(x)\tilde{v}(0,t), \tag{4}$$
$$\partial_t \hat{v}(x,t) = \lambda_2 \partial_x \hat{v}(x,t) + c_2(x)\hat{u}(x,t) + p_2(x)\tilde{v}(0,t), \tag{5}$$

with boundary conditions

$$\hat{u}(0,t) = qv(0,t), \quad \hat{v}(\ell,t) = \rho\hat{u}(\ell,t) + U(t), \tag{6}$$

and initial conditions such that $(\hat{u}^0,\ \hat{v}^0)^T \in L^2((0,\ell);\mathbb{R}^2)$.

The functions $p_1(x)$ and $p_2(x)$ are the observer output injection gains, which are to be determined through backstepping design to ensure the convergence of the estimated states to the plant states. It can be easily verified that the dynamics of the observer errors satisfy

$$\partial_t \tilde{u}(x,t) = -\lambda_1 \partial_x \tilde{u}(x,t) + c_1(x)\tilde{v}(x,t) - p_1(x)\tilde{v}(0,t), \tag{7}$$
$$\partial_t \tilde{v}(x,t) = \lambda_2 \partial_x \tilde{v}(x,t) + c_2(x)\tilde{u}(x,t) - p_2(x)\tilde{v}(0,t), \tag{8}$$

with boundary conditions

$$\tilde{u}(0,t) = 0, \quad \tilde{v}(\ell,t) = \rho\tilde{u}(\ell,t), \tag{9}$$

where the initial conditions satisfy $(\tilde{u}^0,\ \tilde{v}^0)^T \in L^2((0,\ell);\mathbb{R}^2)$.

Consider the following observer error backstepping transformations:

$$\tilde{u}(x,t) = \tilde{\alpha}(x,t) - \int_0^x P^{\alpha\alpha}(x,\xi)\tilde{\alpha}(\xi,t)d\xi - \int_0^x P^{\alpha\beta}(x,\xi)\tilde{\beta}(\xi,t)d\xi, \tag{10}$$
$$\tilde{v}(x,t) = \tilde{\beta}(x,t) - \int_0^x P^{\beta\alpha}(x,\xi)\tilde{\alpha}(\xi,t)d\xi - \int_0^x P^{\beta\beta}(x,\xi)\tilde{\beta}(\xi,t)d\xi, \tag{11}$$

defined over the triangular domain $0 \le \xi \le x \le \ell$. The output gain terms are chosen as

$$p_1(x) = -\lambda_2 P^{\alpha\beta}(x,0), \quad p_2(x) = -\lambda_2 P^{\beta\beta}(x,0).$$

Hence, the observer error system (7)–(9) is transformed into the following target system:

$$\partial_t \tilde{\alpha}(x,t) = -\lambda_1 \partial_x \tilde{\alpha}(x,t), \tag{12}$$
$$\partial_t \tilde{\beta}(x,t) = \lambda_2 \partial_x \tilde{\beta}(x,t), \tag{13}$$

with boundary conditions

$$\tilde{\alpha}(0,t) = 0, \quad \tilde{\beta}(\ell,t) = \rho\tilde{\alpha}(\ell,t). \tag{14}$$

The inverse transformations of (10), (11) are given by

$$\tilde{\alpha}(x,t) = \tilde{u}(x,t) + \int_0^x R^{uu}(x,\xi)\tilde{u}(\xi,t)d\xi + \int_0^x R^{uv}(x,\xi)\tilde{v}(\xi,t)d\xi, \tag{15}$$
$$\tilde{\beta}(x,t) = \tilde{v}(x,t) + \int_0^x R^{vu}(x,\xi)\tilde{u}(\xi,t)d\xi + \int_0^x R^{vv}(x,\xi)\tilde{v}(\xi,t)d\xi, \tag{16}$$

defined over the triangular domain $0 \le \xi \le x \le \ell$.

In order to derive a stabilizing control law via PDE backstepping considering the observer system (4)–(6), the following backstepping transformations are introduced:

$$\hat{\alpha}(x,t) = \hat{u}(x,t) - \int_0^x K^{uu}(x,\xi)\hat{u}(\xi,t)d\xi - \int_0^x K^{uv}(x,\xi)\hat{v}(\xi,t)d\xi, \tag{17}$$
$$\hat{\beta}(x,t) = \hat{v}(x,t) - \int_0^x K^{vu}(x,\xi)\hat{u}(\xi,t)d\xi - \int_0^x K^{vv}(x,\xi)\hat{v}(\xi,t)d\xi. \tag{18}$$

The inverse transformations of (17), (18) are given by

$$\hat{u}(x,t) = \hat{\alpha}(x,t) + \int_0^x L^{\alpha\alpha}(x,\xi)\hat{\alpha}(\xi,t)d\xi + \int_0^x L^{\alpha\beta}\hat{\beta}(\xi,t)d\xi, \tag{19}$$
$$\hat{v}(x,t) = \hat{\beta}(x,t) + \int_0^x L^{\beta\alpha}(x,\xi)\hat{\alpha}(\xi,t)d\xi + \int_0^x L^{\beta\beta}(x,\xi)\hat{\beta}(\xi,t)d\xi. \tag{20}$$

The backstepping transformations are defined over the triangular domain $0 \le \xi \le x \le \ell$. Let us choose the control input $U(t)$ as

$$U(t) = \int_0^\ell N^\alpha(\xi)\hat{\alpha}(\xi,t)d\xi + \int_0^\ell N^\beta(\xi)\hat{\beta}(\xi,t)d\xi, \tag{21}$$

where

$$N^\alpha(\xi) = L^{\beta\alpha}(\ell,\xi) - \rho L^{\alpha\alpha}(\ell,\xi), \tag{22}$$
$$N^\beta(\xi) = L^{\beta\beta}(\ell,\xi) - \rho L^{\alpha\beta}(\ell,\xi). \tag{23}$$

It is worth noting that the control input $U(t)$ given by (21) can also be expressed in terms of $\hat{u}(x,t)$ and $\hat{v}(x,t)$ (Somathilake, Rathnayake, & Diagne, 2024).

Then, the observer (4)–(6) gets transformed into the following target system:

$$\partial_t \hat{\alpha}(x,t) = -\lambda_1 \partial_x \hat{\alpha}(x,t) + \bar{p}_1(x)\tilde{\beta}(0,t), \tag{24}$$
$$\partial_t \hat{\beta}(x,t) = \lambda_2 \partial_x \hat{\beta}(x,t) + \bar{p}_2(x)\tilde{\beta}(0,t), \tag{25}$$

with boundary conditions

$$\hat{\alpha}(0,t) = q\hat{\beta}(0,t) + q\tilde{\beta}(0,t), \quad \hat{\beta}(\ell,t) = \rho\hat{\alpha}(\ell,t), \tag{26}$$

where

$$\bar{p}_1(x) = p_1(x) - \int_0^x K^{uu}(x,\xi)p_1(\xi)d\xi - \int_0^x K^{uv}(x,\xi)p_2(\xi)d\xi, \tag{27}$$
$$\bar{p}_2(x) = p_2(x) - \int_0^x K^{vu}(x,\xi)p_1(\xi)d\xi - \int_0^x K^{vv}(x,\xi)p_2(\xi)d\xi. \tag{28}$$

The PDEs that the kernels of the backstepping transformations (10), (11), (15), (16), (17), (18), (19), and (20) satisfy are defined in Somathilake et al. (2024). Additionally, the proof of existence and uniqueness of solutions to the kernel PDEs is given in Vazquez et al. (2011).

Proposition 1. *Subject to Assumption 1, the continuous-time plant and the observer (1)–(3), (4)–(6) with the continuous-time control input (21) is globally exponentially stable in the spatial L^2 norm.*

We refer the readers to Somathilake et al. (2024) for the proof of the above proposition.

From (21), we derive by emulation the following aperiodic sampled-data control signal held constant between events:

$$U_k^\omega(t) := U(t_k^\omega), \tag{29}$$

for all $t \in [t_k^\omega, t_{k+1}^\omega), k \in \mathbb{N}$, $\omega = \{\text{"}c\text{"}, \text{"}p\text{"}, \text{"}s\text{"}\}$. Entities related to CETC, PETC, and STC are labeled by the superscripts "c", "p", and "s" respectively. In subsequent sections, we present event-triggering rules to determine increasing sequences of event times, $I^\omega = \{t_k^\omega\}_{k\in\mathbb{N}}$. The deviation between the sampled-data control (29) and the continuous control (21), referred to as the input holding error, is defined as

$$d(t) := U_k^\omega(t) - U(t), \tag{30}$$

for $t \in [t_k^\omega, t_{k+1}^\omega), k \in \mathbb{N}$. Under the control input $U_k^\omega(t)$, the boundary values (3), (6), and (26) change to

$$v(\ell, t) = \rho u(\ell, t) + U_k^\omega(t), \tag{31}$$

$$\hat{v}(\ell, t) = \rho \hat{u}(\ell, t) + U_k^\omega(t), \tag{32}$$

$$\hat{\beta}(\ell, t) = \rho \hat{\alpha}(\ell, t) + d(t). \tag{33}$$

In the following proposition, we establish the well-posedness of the systems (1)–(3), (4) and (31)–(6), (32) between consecutive events.

Proposition 2. *Let $k \in \mathbb{N}$, and $U_k^\omega(t) \in \mathbb{R}$ be constant between two event times t_k^ω and t_{k+1}^ω. For a given $(u(\cdot, t_k^\omega), v(\cdot, t_k^\omega))^T \in L^2((0,\ell); \mathbb{R}^2)$ and $(\hat{u}(\cdot, t_k^\omega), \hat{v}(\cdot, t_k^\omega))^T \in L^2((0,\ell); \mathbb{R}^2)$, there exist unique solutions such that $(u, v)^T \in \mathcal{C}^0([t_k^\omega, t_{k+1}^\omega]; L^2((0,\ell); \mathbb{R}^2))$ and $(\hat{u}, \hat{v})^T \in \mathcal{C}^0([t_k^\omega, t_{k+1}^\omega]; L^2((0,\ell); \mathbb{R}^2))$ to the systems (1)–(3), (4) and (31)–(6), (32) respectively between two time instants t_k^ω and t_{k+1}^ω.*

The proof of Proposition 2 is similar to Espitia (2020, Proposition 1).

We now proceed to develop the following result on the existence and uniqueness of solutions of the systems (1)–(3), (4) and (31)–(6), (32) with the input (29) for all $t \in \mathbb{R}^+$.

Corollary 1. *Let $k \in \mathbb{N}$, and $U_k^\omega(t) \in \mathbb{R}$ be constant between two event times t_k^ω and t_{k+1}^ω in the sequence of event times $I^\omega = \{t_k^\omega\}_{k\in\mathbb{N}}$, and assume that for all such intervals, there exists a lower bound $\tau_0 > 0$ such that $t_{k+1}^\omega - t_k^\omega \geq \tau_0$. Then, for every initial condition $(u^0, v^0)^T \in L^2((0,\ell); \mathbb{R}^2)$ and $(\hat{u}^0, \hat{v}^0)^T \in L^2((0,\ell); \mathbb{R}^2)$, there exist unique solutions $(u, v)^T \in \mathcal{C}^0(\mathbb{R}^+; L^2((0,\ell); \mathbb{R}^2))$ and $(\hat{u}, \hat{v})^T \in \mathcal{C}^0(\mathbb{R}^+; L^2((0,\ell); \mathbb{R}^2))$ to the systems (1)–(3), (4) and (31)–(6), (32) respectively.*

The proof of the above corollary can be obtained by using Proposition 2 and following (Espitia, 2020, Proposition 1).

Considering an interval $t \in (t_k^\omega, t_{k+1}^\omega), k \in \mathbb{N}$ and using Proposition 2, the following lemma holds for $d(t)$ given by (30).

Lemma 1. *For $d(t)$ given by (30), the following inequality holds for all $t \in (t_k^\omega, t_{k+1}^\omega), k \in \mathbb{N}$:*

$$(\dot{d}(t))^2 \leq \epsilon_0 \|(\hat{\alpha}(\cdot,t), \hat{\beta}(\cdot,t))^T\|^2 + \epsilon_1 \hat{\alpha}^2(\ell, t) + \epsilon_2 \tilde{\beta}^2(0,t) + \epsilon_3 d^2(t), \tag{34}$$

where $\epsilon_0, \epsilon_1, \epsilon_2$, and $\epsilon_3 \geq 0$ are given by

$$\epsilon_0 = 5 \max\left\{\lambda_1^2 \int_0^\ell (\partial_\xi N^\alpha(\xi))^2 d\xi, \lambda_2^2 \int_0^\ell (\partial_\xi N^\beta(\xi))^2 d\xi\right\}, \tag{35}$$

$$\epsilon_1 = 5(\lambda_1 N^\alpha(\ell) - \rho\lambda_2 N^\beta(\ell))^2, \tag{36}$$

$$\epsilon_2 = 5\left(\int_0^\ell \left(N^\alpha(\xi)\bar{p}_1(\xi) + N^\beta(\xi)\bar{p}_2(\xi)\right) d\xi + q\lambda_1 N^\alpha(0)\right)^2, \tag{37}$$

$$\epsilon_3 = 5(\lambda_2 N^\beta(\ell))^2. \tag{38}$$

The proof of Lemma 1 follows the steps in Espitia (2020, Lemma 2) and can be found in Somathilake et al. (2024).

2.2. Continuous-time event-triggered control (CETC)

This section details the CETC triggering mechanism that determines the increasing sequence of event times $I^c = \{t_k^c\}_{k\in\mathbb{N}}$ at which the control input $U_k^c(t)$ is updated by continuously evaluating a triggering function $\Gamma^c(t)$. The sequence I^c is determined by the following rule.

Definition 1. The increasing sequence of event times $I^c = \{t_k^c\}_{k\in\mathbb{N}}$ with $t_0^c = 0$ are determined via the following rule:

$$t_{k+1}^c := \inf\{t \in \mathbb{R} | t > t_k^c, \Gamma^c(t) > 0, k \in \mathbb{N}\}, \tag{39}$$

$$\Gamma^c(t) := \theta d^2(t) + m(t), \tag{40}$$

where $d(t)$ is given by (30). The dynamic variable $m(t)$ evolves according to the ODE

$$\dot{m}(t) = -\eta m(t) + \theta_m d^2(t) - \kappa_0 \|(\hat{\alpha}(\cdot,t), \hat{\beta}(\cdot,t))^T\|^2 - \kappa_1 \hat{\alpha}^2(\ell,t) - \kappa_2 \tilde{\beta}^2(0,t), \tag{41}$$

for $t \in (t_k^c, t_{k+1}^c), k \in \mathbb{N}$ with $m(0) = m^0 < 0$, $m(t_k^{c^-}) = m(t_k^c) = m(t_k^{c^+})$ $k \in \mathbb{N}$. Let $\eta, \theta > 0$ be arbitrary parameters and $\kappa_0, \kappa_1, \kappa_2 > 0$, and $\theta_m > 0$ be event-trigger parameters to be determined.

It should be noted that the CETC design follows the design procedure in Espitia (2020) with the only difference being that the control input is anti-collocated with the measurement.

The event-triggering rule guarantees that $\Gamma^c(t) \leq 0$ for all $t \in [0, F)$, where $F = \sup\{I^c\}$, hence the following lemma holds.

Lemma 2. *Under the CETC approach (29), (39)–(41), the dynamic variable $m(t)$ with $m^0 < 0$ satisfies $m(t) < 0$ for all $t \in [0, F)$, where $F = \sup\{I^c\}$.*

The proof of the above Lemma is similar to Espitia (2020, Lemma 1).

The existence of a minimum dwell-time $\tau > 0$ is shown in the following lemma.

Lemma 3. *Let the CETC events be triggered according to the rule (39)–(41). Furthermore, let $\sigma \in (0,1)$ and θ be free parameters, and $\kappa_0, \kappa_1, \kappa_2 > 0$ satisfy*

$$\theta\epsilon_i = (1-\sigma)\kappa_i, \quad \text{for } i = 0, 1, 2, \tag{42}$$

where $\epsilon_0, \epsilon_1, \epsilon_2$ are given by (35)–(37), respectively. Then, there exists a minimum dwell-time $\tau > 0$ such that $t_{k+1}^c - t_k^c \geq \tau$ for all $k \in \mathbb{N}$.

The proof Lemma 3 can be obtained by following a procedure similar to that in Espitia (2020, Theorem 1). In addition, we can obtain an expression for the minimum dwell-time as given below:

$$\tau = \frac{1}{a}\ln\left(1 + \frac{a\theta\sigma}{(a\theta + \theta_m)(1-\sigma)}\right), \tag{43}$$

$$a = 1 + \epsilon_3 + \eta > 0. \tag{44}$$

We establish the global exponential convergence of closed-loop system (1)–(3), (4)–(6), (29), (31), (32) in the following proposition.

Proposition 3. *Subject to Assumption 1, let $\eta, \theta > 0$, $\sigma \in (0, 1)$ and the parameter θ_m, be selected such that*

$$\theta_m = 2De^{\mu \frac{\ell}{\lambda_2}}, \tag{45}$$

where

$$D = 2Cq^2, \tag{46}$$

$$C > \max\left\{ \frac{\kappa_0}{(\mu-\delta)r}, \frac{\kappa_1}{1 - 4\rho^2 q^2 e^{\mu\left(\frac{\ell}{\lambda_1}+\frac{\ell}{\lambda_2}\right)}} \right\}, \tag{47}$$

$$\mu \in \left(0, \frac{2\lambda_1\lambda_2}{\ell(\lambda_1+\lambda_2)} \ln\left(\frac{1}{2|q\rho|}\right)\right), \quad \delta < \mu, \tag{48}$$

$$r = \min\left\{ \frac{1}{\lambda_1} e^{-\mu\frac{\ell}{\lambda_1}}, \frac{2q^2}{\lambda_2} \right\}, \tag{49}$$

and κ_0, $\kappa_1 > 0$ satisfy (42). Then, under the CETC triggering rule (39)–(41), the observer-based CETC closed-loop system (1)–(3), (4)–(6), (29), (31), (32) has a unique solution $(u, v, \hat{u}, \hat{v})^T \in \mathcal{C}^0(\mathbb{R}^+; L^2((0,\ell); \mathbb{R}^4))$, and the closed-loop system states globally exponentially converge to 0 in the spatial L^2 norm.

Proof. Using Corollary 1 and Lemma 3, we can conclude that the closed-loop system (1)–(3), (4)–(6), (29), (31), (32), has a unique solution $(u, v, \hat{u}, \hat{v})^T \in \mathcal{C}^0(\mathbb{R}^+; L^2((0,\ell); \mathbb{R}^4))$. Consider the following Lyapunov function for the systems (12)–(14) and (24)–(26), (33):

$$W(t) = V_1(t) + V_2(t) - m(t), \tag{50}$$

where

$$V_1(t) = \int_0^\ell \left(\frac{A}{\lambda_1}\tilde{\alpha}^2(x,t)e^{-\mu\frac{x}{\lambda_1}} + \frac{B}{\lambda_2}\tilde{\beta}^2(x,t)e^{\mu\frac{x}{\lambda_2}} \right) dx,$$

$$V_2(t) = \int_0^\ell \left(\frac{C}{\lambda_1}\hat{\alpha}^2(x,t)e^{-\mu\frac{x}{\lambda_1}} + \frac{D}{\lambda_2}\hat{\beta}^2(x,t)e^{\mu\frac{x}{\lambda_2}} \right) dx.$$

By selecting the values of A, B appropriately and D, C, μ as given in (46)–(48), we can show that $\dot{W}(t) \leq -\min\left\{\mu - \delta - \frac{\kappa_0}{Cr}, \eta\right\} W(t)$. Hence, it can be seen that the target systems globally exponentially converge to 0. Using the bounded invertibility of transformations (10), (11), (15), (16), (17), (18), (19), and (20), we can show that the observer-based CETC closed-loop system (1)–(3), (4)–(6), (29), (31), (32) globally exponentially converges to 0 in the spatial L^2 norm. ■

Remark 1. The variables θ and η are free design parameters that can be varied to tune the performance of the controller, in contrast to the CETC design in Espitia (2020), where these parameters are restricted. Also, as evident by the proof of Proposition 3, larger η, larger μ, and smaller δ would result in a higher convergence rate.

3. Periodic event-triggered control (PETC)

Unlike the CETC approach, in PETC, the triggering function $\Gamma^p(t)$ to be designed is only evaluated periodically. An increasing sequence of PETC times, $I^p = \{t_k^p\}_{k\in\mathbb{N}}$, at which the control input $U_k^p(t)$ is updated, is determined according to the following rule:

Definition 2. The increasing sequence of event times $I^p = \{t_k^p\}_{k\in\mathbb{N}}$ with $t_0^p = 0$ is determined via to the following rule:

$$t_{k+1}^p = \inf\{t \in \mathbb{R} | t > t_k^p, \Gamma^p(t) > 0, k \in \mathbb{N}, \\ t = nh, n \in \mathbb{N}, h > 0\}, \tag{51}$$

$$\Gamma^p(t) := \left(e^{ah}(\theta_m + a\theta) - \theta_m\right) d^2(t) + am(t), \tag{52}$$

where $h > 0$ is an appropriate sampling period to be chosen. Let $\eta, \theta > 0$ be arbitrary parameters. The constants a and θ_m are chosen as in (44) and (45) respectively. The function $d(t)$ is given by (30) and $m(t)$ evolves according to (41) with $m(0) = m^0 < 0$, $m(t_k^{p^-}) = m(t_k^p) = m(t_k^{p^+})$ $k \in \mathbb{N}$.

3.1. Sampling period selection and design of the triggering function

Let us first focus on the selection of the sampling period $h > 0$. Assume that triggering according to the PETC triggering rule (51), (52) ensures that the CETC triggering function $\Gamma^c(t)$ given by (40) satisfies $\Gamma^c(t) \leq 0$ for all $t \in \mathbb{R}^+$ along the PETC closed-loop solution. Then, similarly from Lemma 2, it holds that $m(t)$ governed by (41) satisfies $m(t) < 0$ for all $t \in \mathbb{R}^+$. Let an event be triggered at $t = t_k^p$, then from (40), we see that $\Gamma^c(t_k^p) = m(t_k^p) < 0$. Then, due to the existence of a minimum dwell-time, we know that $\Gamma^c(t)$ remains negative at least until $t = t_k^p + \tau$. Therefore, let us select the sampling period h as

$$0 < h \leq \tau. \tag{53}$$

Let us now focus on the design of the periodic event-triggering function $\Gamma^p(t)$.

Proposition 4. *Consider the set of increasing event times $I^p = \{t_k^p\}_{k\in\mathbb{N}}$ with $t_0^p = 0$ generated by the PETC triggering rule (51), (52) with the sampling period $h > 0$ chosen as in (53). Then, the CETC triggering function $\Gamma^c(t)$ given by (40) satisfies the following relation*

$$\Gamma^c(t) \leq \frac{e^{-\eta(t-nh)}}{a}\Big[\left(e^{a(t-nh)}(\theta_m + a\theta) - \theta_m\right) d^2(nh) \\ + am(nh)\Big], \tag{54}$$

for all $t \in [nh, (n+1)h)$, $n \in [t_k^p/h, t_{k+1}^p/h) \cap \mathbb{N}$, $k \in \mathbb{N}$ where $\eta, \theta > 0$ are free parameters. Constants a, θ_m, and κ_i for $i = 0, 1, 2$ satisfy (44), (45), and (42), respectively.

Proof. Consider a time interval $t \in [nh, (n+1)h)$, $n \in [t_k^p/h, t_{k+1}^p/h) \cap \mathbb{N}$, $k \in \mathbb{N}$, note that $d(t)$, $m(t)$, and $\Gamma^c(t)$ are continuous for all $t \in (nh, (n+1)h)$. Taking the time derivative of (40) for $t \in (nh, (n+1)h)$, the following ODE holds:

$$\dot{\Gamma}^c(t) = 2\theta d(t)\dot{d}(t) + \dot{m}(t).$$

Using Young's inequality and (34), (41) we can derive the following relation:

$$\dot{\Gamma}^c(t) \leq \left(1 + \epsilon_3 + \frac{\theta_m}{\theta}\right)\theta d^2(t) - \eta m(t) \\ + (\theta\epsilon_0 - \kappa_0)\,\|(\hat{\alpha}(\cdot,t), \hat{\beta}(\cdot,t))^T\|^2 \\ + (\theta\epsilon_1 - \kappa_1)\,\hat{\alpha}^2(\ell,t) + (\theta\epsilon_2 - \kappa_2)\,\tilde{\beta}^2(0,t).$$

Substituting for $d^2(t)$ using (40) and introducing $\iota(t) \geq 0$ we arrive at the following ODE:

$$\dot{\Gamma}^c(t) = \left(1 + \epsilon_3 + \frac{\theta_m}{\theta}\right)\Gamma^c(t) - \left(a + \frac{\theta_m}{\theta}\right)m(t) \\ - \iota(t) + (\theta\epsilon_0 - \kappa_0)\,\|(\hat{\alpha}(\cdot,t), \hat{\beta}(\cdot,t))^T\|^2 \\ + (\theta\epsilon_1 - \kappa_1)\,\hat{\alpha}^2(\ell,t) + (\theta\epsilon_2 - \kappa_2)\,\tilde{\beta}^2(0,t). \tag{55}$$

Using (40) and (41), we obtain the following ODE

$$\dot{m}(t) = -\kappa_0\|(\hat{\alpha}(\cdot,t), \hat{\beta}(\cdot,t))^T\|^2 - \kappa_1\hat{\alpha}^2(\ell,t) - \kappa_2\tilde{\beta}^2(0,t) \\ + \frac{\theta_m}{\theta}\Gamma^c(t) - \left(\eta + \frac{\theta_m}{\theta}\right)m(t). \tag{56}$$

Define the following matrices

$$\mathbf{z}(t)=\begin{pmatrix}\Gamma^c(t)\\ m(t)\end{pmatrix},\quad \mathbf{A}=\begin{pmatrix}\left(1+\epsilon_3+\frac{\theta_m}{\theta}\right) & \left(-a-\frac{\theta_m}{\theta}\right)\\ \frac{\theta_m}{\theta} & \left(-\eta-\frac{\theta_m}{\theta}\right)\end{pmatrix},$$

$$\mathbf{B}(t)=\begin{pmatrix}(\theta\epsilon_0-\kappa_0)\,\|(\hat{\alpha}(\cdot,t),\hat{\beta}(\cdot,t))^T\|^2\\ +(\theta\epsilon_1-\kappa_1)\,\hat{\alpha}^2(\ell,t)+(\theta\epsilon_2-\kappa_2)\,\tilde{\beta}^2(0,t)-\iota(t)\\ \kappa_0\|(\hat{\alpha}(\cdot,t),\hat{\beta}(\cdot,t))^T\|^2-\kappa_1\hat{\alpha}^2(\ell,t)-\kappa_2\tilde{\beta}^2(0,t)\end{pmatrix},$$

then from (55) and (56) we obtain

$$\dot{\mathbf{z}}(t)=\mathbf{A}\mathbf{z}(t)+\mathbf{B}(t). \tag{57}$$

The solution to (57) for all $t\in[nh,(n+1)h),\ n\in[t_k^p/h,t_{k+1}^p/h)\cap\mathbb{N}, k\in\mathbb{N}$ is

$$\mathbf{z}(t)=e^{\mathbf{A}(t-nh)}\mathbf{z}(nh)+\int_{nh}^{t}e^{\mathbf{A}(t-\xi)}\mathbf{B}(\xi)d\xi.$$

Let $\mathbf{C}=(1\ 0)$. Since $\Gamma^c(t)=\mathbf{C}\mathbf{z}(t)$, $\Gamma^c(t)$ can be calculated as

$$\Gamma^c(t)=\mathbf{C}e^{\mathbf{A}(t-nh)}\mathbf{z}(nh)+\int_{nh}^{t}\mathbf{C}e^{\mathbf{A}(t-\xi)}\mathbf{B}(\xi)d\xi.$$

Finding the eigenvalues and eigenvectors of $\mathbf{A}$, we determine $e^{\mathbf{A}(t)}$. Then, $\mathbf{C}e^{\mathbf{A}(t-\xi)}\mathbf{B}(\xi)$ can be determined to be

$$\begin{aligned}\mathbf{C}e^{\mathbf{A}(t-\xi)}\mathbf{B}(\xi)=&\frac{e^{-\eta(t-\xi)}}{a}\Bigg[-\frac{g(t-\xi)}{\theta}e^{-\eta(t-\xi)}\iota(\xi)\\ &(g(t-\xi)\epsilon_0-\kappa_0 a)\|(\hat{\alpha}(\cdot,\xi),\hat{\beta}(\cdot,\xi))^T\|^2\\ &+(g(t-\xi)\epsilon_1-\kappa_1 a)\hat{\alpha}^2(\ell,\xi)+(g(t-\xi)\epsilon_2-\kappa_2 a)\tilde{\beta}^2(0,\xi)\Bigg],\end{aligned}$$

where the increasing function $g(t)>0$ is given by

$$g(t)=(e^{at}(\theta_m+a\theta)-\theta_m).$$

Now, for $nh\le\xi\le t\le(n+1)h$, using (42) and (43), $g(t-\xi)\epsilon_i-\kappa_i a$ for $i=0,1,2$ can be shown to satisfy

$$\begin{aligned}g(t-\xi)\epsilon_i-\kappa_i a\le& g(h)\epsilon_i-\kappa_i a,\\ \le&\epsilon_i\left[e^{ah}(\theta_m+a\theta)-\left(\theta_m+\frac{a\theta}{1-\sigma}\right)\right],\\ \le&\epsilon_i(\theta_m+\theta a)(e^{ah}-e^{a\tau}).\end{aligned}$$

Since $h\le\tau$, $(e^{ah}-e^{a\tau})\le 0$. Thus, it can be seen that $g(t-\xi)\epsilon_i-\kappa_i a\le 0$ for $i=0,1,2$. Therefore, we have that $\mathbf{C}e^{\mathbf{A}(t-\xi)}\mathbf{B}(\xi)\le 0$ leading to the following inequality:

$$\begin{aligned}\Gamma^c(t)\le&\mathbf{C}e^{\mathbf{A}(t-nh)}\mathbf{z}(nh)\\ \le&\frac{e^{-\eta(t-nh)}}{a}\Bigg[\left(\frac{\theta_m}{\theta}(e^{a(t-nh)}-1)+ae^{a(t-nh)}\right)\Gamma^c(nh)\\ &+\left(a+\frac{\theta_m}{\theta}\right)(1-e^{a(t-nh)})m(nh)\Bigg].\end{aligned}$$

Substituting for $\Gamma^c(nh)$ using (40), we obtain (54), which concludes the proof. ■

Finally, inspired by the relation (54), let us define the periodic event-triggering function $\Gamma^p(t)$ as in (52).

3.2. Convergence of the closed-loop system under PETC

Using the PETC triggering rule (51), (52), we establish the global exponential convergence of the observer-based PETC closed-loop system (1)–(3), (31), (4)–(6), (32) with the control input $U_k^p(t)$ given by (29).

Lemma 4. *Under the PETC triggering rule (51), (52) with a sample period h chosen as in (53), the CETC triggering function $\Gamma^c(t)$ given by (40) and the dynamic variable $m(t)$ governed by (41) satisfy $\Gamma^c(t)\le 0$ and $m(t)<0$ for all $t\in\mathbb{R}^+$.*

Proof. Assume that two successive events are triggered at $t=t_k^p$ and $t=t_{k+1}^p$, $k\in\mathbb{N}$ under the PETC triggering rule (51), (52) with a sampling period of h and $m(t_k^p)<0$. Since $d(t_k^p)=0$, we have from (40) that $\Gamma^c(t_k^p)=m(t_k^p)<0$ and from (52) that $\Gamma^p(t_k^p)=am(t_k^p)<0$. Due to the periodic nature of the triggering mechanism, we evaluate $\Gamma^p(t)$ at each $t=nh$, $n\in[t_k^p/h,t_{k+1}^p/h)\cap\mathbb{N}$ and events are triggered only if $\Gamma^p(nh)>0$. Consider the inequality (54) when $t\in[nh,(n+1)h)$. Since $e^{a(t-nh)}$ is an increasing function of t, we have

$$\begin{aligned}\Gamma^c(t)\le&\frac{e^{-\eta(t-nh)}}{a}\Big[\left(e^{ah}(\theta_m+a\theta)-\theta_m\right)d^2(nh)\\ &+am(nh)\Big]\le\frac{e^{-\eta(t-nh)}}{a}\Gamma^p(nh).\end{aligned}$$

Therefore, $\Gamma^p(nh)\le 0$ implies that $\Gamma^c(t)\le 0$ for all $t\in[nh,(n+1)h)$. Hence, if $\Gamma^p(t)\le 0$ at a certain time, $\Gamma^c(t)$ remains non-positive at least until the next evaluation of the triggering function. Since the next time at which $\Gamma^p(t)>0$ is at $t=t_{k+1}^p$, we know that $\Gamma^c(t)\le 0$ at least until $t=t_{k+1}^{p^-}$. Therefore, from Lemma 2, $m(t)<0$ for $t\in[t_k^p,t_{k+1}^p)$ and by definition, $m(t_{k+1}^{p^-})=m(t_{k+1}^p)=m(t_{k+1}^{p^+})$, leading to $m(t_{k+1}^p)<0$. Since an event is triggered at $t=t_{k+1}^p$, $d(t_{k+1}^p)=0$, resulting in $\Gamma^c(t_{k+1}^p)=m(t_{k+1}^p)<0$, $\Gamma^p(t_{k+1}^p)=am(t_{k+1}^p)<0$. Applying this reasoning for all intervals in I^p and noting that $m^0<0$, we can conclude that $\Gamma^c(t)<0$ and $m(t)<0$ for all $t\in\mathbb{R}^+$. ■

Subsequently, we establish the global exponential convergence of the closed-loop system in the following theorem.

Theorem 1. *Subject to Assumption 1, let $\eta,\theta>0$, $\sigma\in(0,1)$ and the parameters a, θ_m be determined as in (44), (45) respectively. Then, under the PETC triggering rule (51), (52) with the sampling period $h>0$ chosen as in (53), the observer-based PETC closed-loop system (1)–(3), (4)–(6), (29), (31), (32) has a unique solution $(u,v,\hat{u},\hat{v})^T\in\mathcal{C}^0(\mathbb{R}^+;L^2((0,\ell);\mathbb{R}^4))$, and the closed-loop system states globally exponentially converge to 0 in the spatial L^2 norm.*

Proof. Using Corollary 1 and noting that the triggering function is evaluated periodically with a period h, which makes the closed-loop system inherently Zeno-free, we can conclude that the closed-loop system (1)–(3), (4)–(6), (29), (31), (32) has a unique solution $(u,v,\hat{u},\hat{v})^T\in\mathcal{C}^0(\mathbb{R}^+;L^2((0,\ell);\mathbb{R}^4))$. Following Lemma 4, we know that $\Gamma^c(t)\le 0$ and $m(t)<0$ for all $t\in\mathbb{R}^+$ along the PETC closed-loop solution. Therefore, using the same arguments used in Proposition 3, we can conclude that the closed-loop system (1)–(3), (4)–(6), (29), (31), (32), globally exponentially converges to 0 in the spatial L^2 norm. ■

4. Self-triggered control (STC)

In this section, we propose an observer-based STC approach. Unlike the previously proposed CETC and PETC methods, which require evaluating a triggering function to update the control input, the STC approach determines the next event time at the current event time. It does so by using continuously available measurements and predicting an upper bound of the closed-loop system state. Consequently, STC proactively determines event times, whereas both CETC and PETC reactively determine event times.

Before proceeding with the design, we assume the following regarding the initial data.

Assumption 2. The initial conditions of the observer error system given by (7)–(9) satisfy

$$\tilde{u}^2(x,0)\le\phi_u,\quad \tilde{v}^2(x,0)\le\phi_v,$$

for all $x \in [0, \ell]$ for some known arbitrary constants $\phi_u, \phi_v > 0$.

The increasing sequence of event times $I^s = \{t_k^s\}_{k\in\mathbb{N}}$ at which the control input is updated is determined by the following rule.

Definition 3. The increasing sequence of event times $I^s = \{t_k^s\}_{k\in\mathbb{N}}$ with $t_0^s = 0$ is determined via to the following rule:

$$t_{k+1}^s = t_k^s + G(t_k^s), \tag{58}$$

where

$$G(t) = \max\{\tau, \bar{G}(t)\}, \tag{59}$$

$$\bar{G}(t) = \frac{1}{\varrho+\eta}\ln\left(\frac{\theta_m \mathcal{F}(t) - m(t)(\varrho+\eta)}{\mathcal{F}(t)(\theta(\varrho+\eta)+\theta_m)}\right), \tag{60}$$

$$\mathcal{F}(t) = r_d\left(2\bar{V}_2(t) + \frac{2r_d\bar{D}e^{\bar{\mu}\frac{\ell}{\lambda_2}}\bar{V}_2(t)+\phi(t)}{\varrho}\right), \tag{61}$$

$$\bar{V}_2(t) = \int_0^\ell \left(\frac{\bar{C}}{\lambda_1}\hat{\alpha}^2(x,t)e^{-\bar{\mu}\frac{x}{\lambda_1}} + \frac{\bar{D}}{\lambda_2}e^{\bar{\mu}\frac{x}{\lambda_2}}\hat{\beta}^2(x,t)\right)dx, \tag{62}$$

$$\phi(t) = (2\bar{C}q^2 + \bar{P}_{V_2})\phi_0(t), \quad \bar{C} = 1, \quad \bar{D} = 2q^2, \tag{63}$$

$$\bar{\mu} = \frac{2\lambda_1\lambda_2}{\ell(\lambda_1+\lambda_2)}\ln\left(\frac{1}{2|q\rho|}\right), \tag{64}$$

$$\phi_0(t) = \begin{cases}\max\{\rho^2\phi_\alpha, \phi_\beta\} & t \le \frac{\ell}{\lambda_1}+\frac{\ell}{\lambda_2}\\ 0 & t > \frac{\ell}{\lambda_1}+\frac{\ell}{\lambda_2},\end{cases} \tag{65}$$

$$\bar{P}_{V_2} = \bar{\delta}\int_0^\ell \left(\frac{\bar{C}}{\lambda_1}e^{-\bar{\mu}\frac{x}{\lambda_1}}\bar{p}_1^2(x) + \frac{\bar{D}}{\lambda_2}e^{\bar{\mu}\frac{x}{\lambda_2}}\bar{p}_2^2(x)\right)dx, \tag{66}$$

$$\varrho = \bar{\delta} - \bar{\mu} + 2\bar{D}e^{\bar{\mu}\frac{\ell}{\lambda_2}}, \tag{67}$$

$$r_d = \frac{4\max\left\{\int_0^\ell (N^\alpha(\xi))^2 d\xi, \int_0^\ell (N^\beta(\xi))^2 d\xi\right\}}{\min\left\{\frac{\bar{C}e^{-\bar{\mu}\frac{\ell}{\lambda_1}}}{\lambda_1}, \frac{\bar{D}}{\lambda_2}\right\}}, \tag{68}$$

with $\bar{\delta} > 0$ chosen such that $\varrho > 0$ and ϕ_α and ϕ_β being known constants. Let $\eta, \theta > 0$ be arbitrary parameters. Furthermore θ_m is given by (45). The dynamic variable $m(t)$ evolves according to (41) with $m(0) = m^0 < 0$, $m(t_k^{s^-}) = m(t_k^s) = m(t_k^{s^+})$ $k \in \mathbb{N}$.

4.1. Design of the positive function $G(t)$

The function $G(t)$ is determined such that updating control inputs at events generated by the STC triggering rule (58)–(68) ensures the CETC triggering function $\Gamma^c(t)$ given by (40) satisfies $\Gamma^c(t) \le 0$ for all $t \in \mathbb{R}^+$. Towards this, we first derive upper bounds for the variables $d^2(t)$ and $m(t)$ between two consecutive event times t_k^s and t_{k+1}^s.

Lemma 5. *For $d(t)$ given by (30), and for $m(t)$ satisfying (41) with $m(0) = m^0 < 0$, $m(t_k^{s^-}) = m(t_k^s) = m(t_k^{s^+})$ $k \in \mathbb{N}$, the following inequalities hold:*

$$d^2(t) < \mathcal{F}(t_k^s)e^{\varrho(t-t_k^s)}, \tag{69}$$

$$m(t) < e^{-\eta(t-t_k^s)}m(t_k^s) + \frac{\theta_m\mathcal{F}(t_k^s)e^{-\eta(t-t_k^s)}}{\varrho+\eta}\left(e^{(\varrho+\eta)(t-t_k^s)} - 1\right), \tag{70}$$

for all $t \in [t_k^s, t_{k+1}^s)$, $k \in \mathbb{N}$, with $\varrho > 0$ in (67).

Proof. Differentiating the function (62) with respect to time for $t \in [t_k^s, t_{k+1}^s)$, $k \in \mathbb{N}$ and using (24)–(26), (33), the following expression can be obtained:

$$\begin{aligned}\dot{\bar{V}}_2(t) =& 2\tilde{\beta}(0,t)\int_0^\ell \left(\frac{\bar{C}}{\lambda_1}\bar{p}_1(x)e^{-\bar{\mu}\frac{x}{\lambda_1}} + \frac{\bar{D}}{\lambda_2}\bar{p}_2(x)e^{\bar{\mu}\frac{x}{\lambda_2}}\right)dx\\ &- \bar{\mu}\bar{V}_2(t) - \bar{C}\left(e^{-\bar{\mu}\frac{\ell}{\lambda_1}}\hat{\alpha}^2(\ell,t) - \hat{\alpha}^2(0,t)\right)\\ &+ \bar{D}\left(e^{\bar{\mu}\frac{\ell}{\lambda_2}}(\rho\hat{\alpha}(\ell,t)+d(t))^2 - \hat{\beta}^2(0,t)\right).\end{aligned}$$

Then, applying Young's inequality, we can obtain the following where $\bar{\delta} > 0$ and $\bar{P}_{V_2}$ is given in (66):

$$\begin{aligned}\dot{\bar{V}}_2(t) \le& (\bar{\delta} - \bar{\mu})\bar{V}_2(t) + 2\bar{D}e^{\bar{\mu}\frac{\ell}{\lambda_2}}d^2(t)\\ &+ \left(-\bar{C}e^{-\bar{\mu}\frac{\ell}{\lambda_2}} + 2\rho^2\bar{D}e^{\bar{\mu}\frac{\ell}{\lambda_1}}\right)\hat{\alpha}^2(\ell,t) + \tilde{\beta}^2(0,t)\bar{P}_{V_2}\\ &+ \left(2\bar{C}q^2 - \bar{D}\right)\hat{\beta}^2(0,t) + 2\bar{C}q^2\tilde{\beta}^2(0,t).\end{aligned}$$

Selecting $\bar{\mu}$ as defined in (64) along with the parameters $\bar{C}, \bar{D}$ as given in (63), we obtain the following inequality:

$$\dot{\bar{V}}_2(t) \le (\bar{\delta} - \bar{\mu})\bar{V}_2(t) + 2\bar{D}e^{\bar{\mu}\frac{\ell}{\lambda_2}}d^2(t) + \tilde{\beta}^2(0,t)(2\bar{C}q + \bar{P}_{V_2}). \tag{71}$$

To obtain an upper bound for the solution of $\bar{V}_2(t)$ using (71), we derive the following inequalities for $d^2(t)$ and $\tilde{\beta}^2(0,t)$.

Consider $d(t)$ given by (30). Using Young's inequality and Cauchy–Schwarz inequality, the following approximation can be obtained for $d^2(t)$:

$$\begin{aligned}d^2(t) \le& 4\max\left\{\int_0^\ell (N^\alpha(\xi))^2 d\xi, \int_0^\ell (N^\beta(\xi))^2 d\xi\right\}\\ &\times \left(\|(\hat{\alpha}(\cdot,t), \hat{\beta}(\cdot,t))^T\|^2 + \|(\hat{\alpha}(\cdot,t_k^s), \hat{\beta}(\cdot,t_k^s))^T\|^2\right),\end{aligned}$$

Noting that

$$\min\left\{\frac{\bar{C}e^{-\bar{\mu}\frac{\ell}{\lambda_1}}}{\lambda_1}, \frac{\bar{D}}{\lambda_2}\right\}\|(\hat{\alpha}(\cdot,t), \hat{\beta}(\cdot,t))^T\|^2 \le \bar{V}_2(t),$$

the following holds for $d^2(t)$:

$$d^2(t) \le r_d(\bar{V}(t_k^s) + \bar{V}(t)), \tag{72}$$

where r_d is given in (68). Additionally considering the dynamics of the target system (12)–(14), the characteristic solution of the system can be obtained as

$$\tilde{\alpha}(x,t) = \begin{cases}0 & x \le \lambda_1 t\\ \tilde{\alpha}(x-\lambda_1 t, 0) & x > \lambda_1 t,\end{cases} \tag{73}$$

$$\tilde{\beta}(x,t) = \begin{cases}\tilde{\beta}(x+\lambda_2 t, 0) & x \le \ell - \lambda_2 t\\ \rho\tilde{\alpha}\left(\ell + \frac{\lambda_1}{\lambda_2}(\ell - x) - \lambda_1 t, 0\right) & x > \ell - \lambda_2 t.\end{cases} \tag{74}$$

From Assumption 2, using the transformations (15), (16), Young's inequality, and Cauchy–Schwarz inequality, the following inequality can be obtained: $\tilde{\alpha}^2(x,0) \le \phi_\alpha$, $\tilde{\beta}^2(x,0) \le \phi_\beta$, where ϕ_α and ϕ_β are given by

$$\begin{aligned}\phi_\alpha =& 3\max_{x\in[0,\ell]}\left\{\phi_u + \phi_u x\int_0^x (R^{uu}(x,\xi))^2 d\xi\right.\\ &\left.+ \phi_v x\int_0^x (R^{uv}(x,\xi))^2 d\xi\right\},\\ \phi_\beta =& 3\max_{x\in[0,\ell]}\left\{\phi_v + \phi_u x\int_0^x (R^{vu}(x,\xi))^2 d\xi\right.\\ &\left.+ \phi_v x\int_0^x (R^{vv}(x,\xi))^2 d\xi\right\}.\end{aligned}$$

From the solution of $\tilde{\alpha}(x,t)$ and $\tilde{\beta}(x,t)$ given by (73), (74), it is clear that for $t \ge \frac{\ell}{\lambda_1} + \frac{\ell}{\lambda_2}$, $\tilde{\alpha}(x,t) = 0$ and $\tilde{\beta}(x,t) = 0$. Also, $\tilde{\beta}^2(0,t) \le \max\{\rho^2\phi_\alpha, \phi_\beta\}$ for $t < \frac{\ell}{\lambda_1} + \frac{\ell}{\lambda_2}$. Hence $\tilde{\beta}(0,t)$ is bounded for all $t \ge 0$ as

$$\tilde{\beta}^2(0,t) \le \phi_0(t). \tag{75}$$

Since the $\phi_0(t)$ given by (65) is a non-increasing function of t and since $t \in [t_k^s, t_{k+1}^s)$, (75) still holds for R.H.S. at $t = t_k^s$. Substituting $d^2(t)$ from (72) and $\tilde{\beta}^2(0,t)$ from (75) to (71) and at $\phi_0(t) = \phi_0(t_k^s)$, we obtain the following expression:

$$\dot{\bar{V}}_2(t) \le \varrho \bar{V}_2(t) + 2r_d\bar{D}e^{\bar{\mu}\frac{\ell}{\lambda_2}}\bar{V}_2(t_k^s) + \phi(t_k^s),$$

where ϱ and $\phi(t)$ are defined in (63) and (67) respectively. Using the comparison principle, one gets the following estimate:

$$\bar{V}_2(t) < \left(\bar{V}_2(t_k^s) + \frac{2r_d\bar{D}e^{\bar{\mu}\frac{\ell}{\lambda_2}}\bar{V}_2(t_k^s) + \phi(t_k^s)}{\varrho}\right)e^{\varrho(t-t_k^s)}. \tag{76}$$

Using (72) and (76), we derive the estimate (69). Next, using (41) and (69), the following inequality can be derived

$$\dot{m}(t) < -\eta m(t) + \theta_m \mathcal{F}(t_k^s)e^{\varrho(t-t_k^s)}.$$

Using the comparison principle, the estimate (70) can be obtained. ∎

Consider the time period $t \in [t_k^s, t_{k+1}^s)$, $k \in \mathbb{N}$. Assume that $m(t_k^s) < 0$. Since an event is triggered at $t = t_k^s$, we know that $d(t_k^s) = 0$, then, from (40), we know that $\Gamma^c(t_k^s) = m(t_k^s) < 0$. Using (40), (69), and (70), we obtain

$$\begin{aligned}\Gamma^c(t) <& \theta\mathcal{F}(t_k^s)e^{\varrho(t-t_k^s)} + e^{-\eta(t-t_k^s)}m(t_k^s)\\ &+ \frac{\theta_m\mathcal{F}(t_k^s)e^{-\eta(t-t_k^s)}}{\varrho+\eta}\left(e^{(\varrho+\eta)(t-t_k^s)} - 1\right).\end{aligned} \tag{77}$$

R.H.S. of (77) is an increasing function of t. Assume that there exists a time $t_k^{s^*} > t_k^s$ such that the following expression hold:

$$\begin{aligned}&\theta\mathcal{F}(t_k^s)e^{\varrho(t_k^{s*}-t_k^s)} + e^{-\eta(t_k^{s^*}-t_k^s)}m(t_k^s)\\ &+ \frac{\theta_m\mathcal{F}(t_k^s)e^{-\eta(t_k^{s*}-t_k^s)}}{\varrho+\eta}\left(e^{(\varrho+\eta)(t_k^{s^*}-t_k^s)} - 1\right) = 0.\end{aligned}$$

Solving for t_k^{s*}, we get $t_k^{s*} - t_k^s = \bar{G}(t_k^s)$ where $\bar{G}(t)$ is given by (60). Since, $t_k^{s*} - t_k^s > \tau$ is not guaranteed to be true, we define $G(t)$ as in (59).

4.2. Convergence of the closed-loop system under STC

Under the STC triggering rule (58)–(68), we establish global exponential convergence of the observer-based system (1)–(3), (31), (4)–(6), (32) with the control input $U_k^s(t)$ given in (29). Prior to that, we present the following result that is crucial for proving the main result presented in Theorem 2.

Lemma 6. *Under the STC triggering rule (58)–(68), the CETC triggering function $\Gamma^c(t)$ given by (40) and the dynamic variable $m(t)$ governed by (41) satisfy $\Gamma^c(t) \le 0$ and $m(t) < 0$ for all $t \in \mathbb{R}^+$.*

Proof. Assume that two successive events are triggered at $t = t_k^s$ and $t = t_{k+1}^s$, $k \in \mathbb{N}$ under the STC triggering rule (58)–(68) and $m(t_k^s) < 0$. Since $d(t_k^s) = 0$, from (40), $\Gamma^c(t_k^s) = m(t_k^s) < 0$. According to the definition of the STC triggering rule, we have that $t_{k+1}^s = t_k^s+\tau$ if $\bar{G}(t_k^s) \le \tau$ or $t_{k+1}^s = t_k^s+\bar{G}(t_k^s)$ if $\bar{G}(t_k^s) > \tau$. Since τ defined in (43) is the minimum dwell-time, if $t_{k+1}^s = t_k^s + \tau$, we know that $\Gamma^c(t)$ remains non positive until $t = t_{k+1}^{s-}$. Next consider the instance where $t_{k+1}^s = t_k^s + \bar{G}(t_k^s)$. From (77), for $t = t_{k+1}^s$, $\bar{G}(t_k^s)$ is such that

$$\begin{aligned}&\Gamma^c(t_{k+1}^s) < \theta\mathcal{F}(t_k^s)e^{\varrho\bar{G}(t_k^s)} + e^{-\eta\bar{G}(t_k^s)}m(t_k^s)\\ &+ \frac{\theta_m\mathcal{F}(t_k^s)e^{-\eta(\bar{G}(t_k^s))}}{\varrho+\eta}\left(e^{(\varrho+\eta)(\bar{G}(t_k^s))} - 1\right) = 0,\end{aligned}$$

therefore, $\Gamma^c(t_{k+1}^s) < 0$, and since the upper bound for $\Gamma^c(t)$ in (77) is an increasing function of t, $\Gamma^c(t) < 0$ for all $t \in [t_k^s, t_{k+1}^s)$. Therefore, for the STC condition given in (58)–(68), $\Gamma^c(t)$ remains non-positive for $t \in [t_k^s, t_{k+1}^s)$, then similarly from Lemma 2, we can conclude that $m(t) < 0$ for $t \in [t_k^s, t_{k+1}^s)$. By definition, $m(t_{k+1}^{s-}) = m(t_{k+1}^s) = m(t_{k+1}^{s+})$ leading to $m(t_{k+1}^s) < 0$. Since an event is triggered at $t = t_{k+1}^s$, $d(t_{k+1}^s) = 0$, resulting in $\Gamma^c(t_{k+1}^s) = m(t_{k+1}^s) < 0$. Applying this reasoning for all intervals in I^s and noting that $m^0 < 0$, we can conclude that $\Gamma^c(t) < 0$ and $m(t) < 0$ for all $t \in \mathbb{R}^+$. ∎

Note that in light of the results of Lemma 6, $\bar{G}(t)$ in (60) exist for all $t \in I^s$. Subsequently, we establish the global exponential convergence of the closed-loop system in the following theorem.

Theorem 2. *Subject to Assumption 1, let $\eta, \theta > 0$, $\sigma \in (0, 1)$ and the parameters τ, θ_m be defined as in (43), (45) respectively. Then, under the STC triggering rule (58)–(68), the observer-based STC closed-loop system (1)–(3), (4)–(6), (29), (31), (32) has a unique solution $(u, v, \hat{u}, \hat{v})^T \in \mathcal{C}^0(\mathbb{R}^+; L^2((0, \ell); \mathbb{R}^4))$, and the closed-loop system states exponentially converge to 0 in the spatial L^2 norm.*

Proof. Using Corollary 1 and noting that according to the triggering rule (58)–(68) the time between two events is at least τ, which excludes Zeno behavior, we can conclude that the system (1)–(3), (4)–(6), (29), (31), (32) has a unique solution $(u, v, \hat{u}, \hat{v})^T \in \mathcal{C}^0(\mathbb{R}^+; L^2((0, \ell); \mathbb{R}^4))$. Following Lemma 6, we know that $\Gamma^c(t) \le 0$ and $m(t) < 0$ for all $t \in \mathbb{R}^+$. Therefore, using the same arguments used in Proposition 3, we can conclude that the closed-loop system (1)–(3), (4)–(6), (29), (31), (32), exponentially converges to 0 in the spatial L^2 norm. ∎

5. Boundary control of shallow water wave equations

5.1. The Saint-Venant equations

The Saint-Venant model for a canal breach of unit width, which expresses the conservation of mass and momentum assuming that the depth of the incompressible flow is much smaller than the horizontal length scale, is given below:

$$\partial_t H + \partial_x(HV) = 0, \tag{78}$$

$$\partial_t V + \partial_x\left(\frac{V^2}{2} + gH\right) + \left(\frac{C_f V^2}{H} - gS_b\right) = 0, \tag{79}$$

where $H(x, t)$ represents the water depth, $V(x, t)$ is the horizontal water velocity, and g is the constant acceleration of gravity. The term S_b is the constant bottom slope of the channel bed. The constant friction coefficient C_f plays a central role in modulating the fluid's behavior under gravitational influence and resistance posed by the channel. Assume that the flow rate upstream is a known constant Q_0, and an underflow sluice gate is used at the downstream boundary, hence we obtain the following boundary conditions:

$$H(0, t)V(0, t) = Q_0, \tag{80}$$

$$H(\ell, t)V(\ell, t) = k_G\sqrt{2g}U_\ell(t)\sqrt{H(\ell, t) - H_\ell}, \tag{81}$$

where k_G represents the constant discharge coefficient of the gate, H_ℓ is the constant water level beyond the gate, and U_ℓ is the gate opening height which can be controlled to regulate water dynamics in the canal. The constant equilibrium states of $H(x, t)$ and $V(x, t)$ are denoted by H_{eq} and V_{eq}, respectively. For the physical stationary states of interest, it is assumed that both H_{eq} and V_{eq} are positive. Let the following assumptions hold for the system.

Assumption 3. The constant bottom slope S_b and the constant equilibrium states H_{eq}, V_{eq} are such that $S_b = \frac{C_f V_{eq}^2}{g H_{eq}}$.

Assumption 4. The steady states of the system, particularly in scenarios involving navigable rivers and fluvial regimes, the following subcritical condition holds: $gH_{eq} > V_{eq}^2$.

Consider the following coordinate transformation:

$$\begin{pmatrix} u \\ v \end{pmatrix} = \begin{pmatrix} e^{\frac{\gamma_1}{\lambda_1}x} & 0 \\ 0 & e^{-\frac{\gamma_2}{\lambda_2}x} \end{pmatrix} \begin{pmatrix} \sqrt{\frac{g}{H_{eq}}} & 1 \\ -\sqrt{\frac{g}{H_{eq}}} & 1 \end{pmatrix} \begin{pmatrix} H - H_{eq} \\ V - V_{eq} \end{pmatrix}. \tag{82}$$

Subsequently, we linearize the system (78)–(81) around the equilibrium point and use the transformation (82) with known constants γ_1 and γ_2 to represent the linearized system decoupled along its characteristic velocities $\lambda_1 = V_{eq} + \sqrt{gH_{eq}}$ and $-\lambda_2 = V_{eq} - \sqrt{gH_{eq}}$. Under Assumption 4, we observe that $\lambda_1, \lambda_2 > 0$. This leads to a system identical to (1)–(3) with known $c_1(x)$, $c_2(x)$, q, and ρ (see Somathilake et al., 2024).

5.2. Numerical simulations

The simulations for CTC, CETC, PETC, and STC detailed in Section 2–4 respectively are carried out for the one-dimensional shallow water equations given above. The model parameters are defined as $g = 9.81$ m/s^2, $\ell = 10$ m, $C_f = 0.2$, $H_{eq} = 2$ m, $V_{eq} = 1$ m/s, and $H_\ell = 0.1$ m such that the boundary conditions satisfy Assumption 1. In addition, we define $k_G = 0.6$. The initial conditions for the system are selected such that $H(x, 0) = H_{eq} - \sin(\pi \frac{x}{\ell})$, $V(x, 0) = V_{eq} + 0.5\sin(3\pi \frac{x}{\ell})$ along with the initial conditions of the observer states in the characteristic coordinates as $\hat{u}(x, 0) = 0$, $\hat{v}(x, 0) = 0$. The bounds in Assumption 2 are taken as $\phi_u = 8.6872$ and $\phi_v = 3.1664$.

Subsequently, consider the selection of the event-triggering parameters. Select $\mu = 0.016$ such that (48) is satisfied. The tuning parameters $\delta < \mu$, $m^0 < 0$, $\eta > 0$, $\theta > 0$, and $\sigma \in (0, 1)$ are selected as 0.014, -1, 0.001, 1, and 0.99 respectively. Thereafter we select $C = 413.4211$ from (47) and $\bar{\delta} = 10^{-4}$ such that $\varrho > 0$. We obtain a minimum dwell-time of $\tau = 0.13323$ s and the sampling period $0 < h \leq \tau$ in the PETC design is selected as $h = 0.13$ s. The time and spatial step sizes used in PDE discretization are $\Delta t = 0.0001$ s and $\Delta x = 0.05$ m, respectively. The kernel PDEs are solved using the method proposed in Anfinsen and Aamo (2019) [Appendix F].

The variation of the L^2 norms of the characteristic coordinates $\|(u(\cdot, t), v(\cdot, t))^T\|$, over time is depicted in Fig. 1(a) for the open-loop (OL) system and under the CTC, CETC, PETC, and STC mechanisms. The corresponding control inputs for the triggering mechanisms are shown in Fig. 1(b). The dwell-times for CETC and PETC are shown in Fig. 2(a), and the dwell-times for STC are shown in Fig. 2(b). The dwell-times for STC are much shorter than the dwell-times for CETC and PETC because, unlike CETC and PETC, the STC approach proactively computes the next event time by predicting the state evolution. This results in a more conservative sampling schedule. Due to frequent control updates, the closed-loop signals under STC follow a trajectory closer to those under CTC, as seen in Fig. 1(a). In contrast, CETC and PETC approaches are less conservative in determining the triggering times; therefore, the norms converge to zero over a longer period but with less frequent control updates.

6. Concluding remarks

This article has presented an anti-collocated observer-based periodic event-triggered and self-triggered boundary control for a class of 2×2 hyperbolic PDEs with reflection terms at the boundaries. The proposed PETC approach evaluates an appropriately designed function periodically to determine event times and is equipped with an explicitly defined upper bound for the sampling period. In contrast, the STC approach employs a positively lower-bounded function, which is evaluated at an event to determine the next event time. Both approaches eliminate the need for continuous monitoring of a triggering function required in the CETC approach while still preserving global exponential convergence to zero in the spatial L^2 norm. We have established the well-posedness of the closed-loop system under the proposed control strategies. The proposed control strategies have been employed to control the linearized Saint-Venant equations, which describe the flow of water in an open channel with a constant inflow of water at the upstream boundary and a sluice gate at the downstream boundary. Since the control input is transmitted only at event times, the communication bandwidth is utilized effectively and can be freed for other tasks.

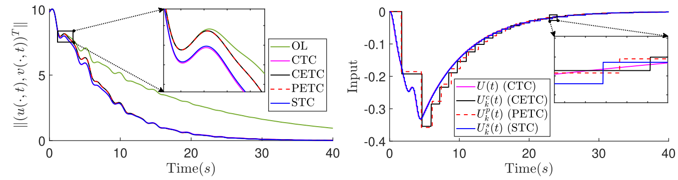

(a) Variation of the spatial L^2 norm of characteristic coordinates with time. (b) Variation of the control inputs with time.

Fig. 1. L^2 norm of characteristics and control inputs.

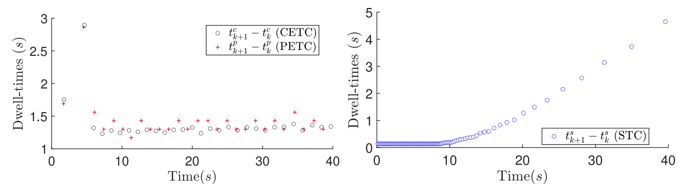

(a) CETC and PETC dwell-times. (b) Dwell-times under STC.

Fig. 2. Dwell times under event-triggered strategies.

References

Anfinsen, H., & Aamo, O. M. (2019). *Adaptive control of hyperbolic PDEs*. Springer.

Anfinsen, H., Diagne, M., Aamo, O. M., & Krstic, M. (2016). An adaptive observer design for $n + 1$ coupled linear hyperbolic PDEs based on swapping. *IEEE Transactions on Automatic Control*, *61*(12), 3979–3990.

Anfinsen, H., Diagne, M., Aamo, O. M., & Krstic, M. (2017). Estimation of boundary parameters in general heterodirectional linear hyperbolic systems. *Automatica*, *79*, 185–197.

Bastin, G., & Coron, J.-M. (2011). On boundary feedback stabilization of non-uniform linear 2×2 hyperbolic systems over a bounded interval. *Systems & Control Letters*, *60*(11), 900–906.

Burkhardt, M., Yu, H., & Krstic, M. (2021). Stop-and-go suppression in two-class congested traffic. *Automatica*, *125*, Article 109381.

Coron, J.-M., d'Andréa Novel, B., & Bastin, G. (1999). A Lyapunov approach to control irrigation canals modeled by Saint-Venant equations. In *1999 European control conference* (pp. 3178–3183). IEEE.

Di Meglio, F., Vazquez, R., & Krstic, M. (2013). Stabilization of a system of $n+1$ coupled first-order hyperbolic linear PDEs with a single boundary input. *IEEE Transactions on Automatic Control*, *58*(12), 3097–3111.

Diagne, A., Diagne, M., Tang, S., & Krstic, M. (2017). Backstepping stabilization of the linearized Saint-Venant-Exner model. *Automatica*, *76*, 345–354.

Diagne, M., & Karafyllis, I. (2021). Event-triggered boundary control of a continuum model of highly re-entrant manufacturing systems. *Automatica*, *134*, Article 109902.

Diagne, M., Tang, S.-X., Diagne, A., & Krstic, M. (2017). Control of shallow waves of two unmixed fluids by backstepping. *Annual Reviews in Control*, *44*, 211–225.

Espitia, N. (2020). Observer-based event-triggered boundary control of a linear 2×2 hyperbolic systems. *Systems & Control Letters*, *138*, Article 104668. http://dx.doi.org/10.1016/j.sysconle.2020.104668.

Espitia, N., Karafyllis, I., & Krstic, M. (2021). Event-triggered boundary control of constant-parameter reaction–diffusion PDEs: A small-gain approach. *Automatica*, *128*, Article 109562.

Halleux, J. D., Prieur, C., Coron, J. M., dÂndréa Novel, B., & Bastin, G. (2003). Boundary feedback control in networks of open channels. *Automatica*, *39*(8), 1365–1376.

Hu, L., Di Meglio, F., Vazquez, R., & Krstic, M. (2016). Control of homodirectional and general heterodirectional linear coupled hyperbolic PDEs. *IEEE Transactions on Automatic Control*, *61*(11), 3301–3314.

Ong, P., & Cortés, J. (2023). Performance-barrier-based event-triggered control with applications to network systems. *IEEE Transactions on Automatic Control*.

Rathnayake, B., & Diagne, M. (2024a). Observer-based event-triggered boundary control of the one-phase Stefan problem. *International Journal of Control*, 1–12.

Rathnayake, B., & Diagne, M. (2024b). Observer-based periodic event-triggered and self-triggered boundary control of a class of parabolic PDEs. *IEEE Transactions on Automatic Control*, *69*(12), 8836–8843.

Rathnayake, B., Diagne, M., Cortés, J., & Krstic, M. (2025). Performance-barrier event-triggered control of a class of reaction–diffusion PDEs. *Automatica*, *174*, Article 112181. http://dx.doi.org/10.1016/j.automatica.2025.112181.

Rathnayake, B., Diagne, M., Espitia, N., & Karafyllis, I. (2021). Observer-based event-triggered boundary control of a class of reaction–diffusion PDEs. *IEEE Transactions on Automatic Control*, *67*(6), 2905–2917.

Rathnayake, B., Diagne, M., & Karafyllis, I. (2022). Sampled-data and event-triggered boundary control of a class of reaction–diffusion PDEs with collocated sensing and actuation. *Automatica*, *137*, Article 110026.

Somathilake, E., & Diagne, M. (2024). Output feedback control of suspended sediment load entrainment in water canals and reservoirs. *IFAC-PapersOnLine*, *58*(28), 983–988, The 4th Modeling, Estimation, and Control Conference – 2024.

Somathilake, E., Rathnayake, B., & Diagne, M. (2024). Output feedback periodic event-triggered and self-triggered boundary control of coupled 2×2 linear hyperbolic PDEs. arXiv preprint arXiv:2404.02298.

Vazquez, R., Krstic, M., & Coron, J.-M. (2011). Backstepping boundary stabilization and state estimation of a 2×2 linear hyperbolic system. In *2011 50th IEEE conference on decision and control and European control conference* (pp. 4937–4942).

Wang, J., & Krstic, M. (2022a). Event-triggered adaptive control of a parabolic PDE-ODE cascade with piecewise-constant inputs and identification. *IEEE Transactions on Automatic Control*.

Wang, J., & Krstic, M. (2022b). Event-triggered adaptive control of coupled hyperbolic PDEs with piecewise-constant inputs and identification. *IEEE Transactions on Automatic Control*, *68*(3), 1568–1583.

Yu, H., & Krstic, M. (2022). *Traffic Congestion Control by PDE Backstepping*. Springer.

Zhang, P., Rathnayake, B., Diagne, M., & Krstic, M. (2025). Performance-barrier event-triggered PDE control of traffic flow. *IEEE Transactions on Automatic Control*, 1–16. http://dx.doi.org/10.1109/TAC.2025.3547958.

Eranda Somathilake received his B.Sc. in Mechanical Engineering from the University of Peradeniya, Sri Lanka, in 2020. He is currently pursuing a Ph.D. in the Department of Mechanical and Aerospace Engineering at the University of California, San Diego. His research interests focus on the control of distributed parameter systems, with a particular emphasis on control of river–sediment dynamics.

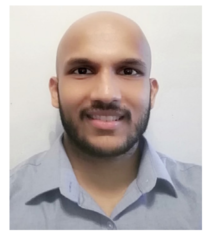

Bhathiya Rathnayake received his B.Sc. in Engineering, specializing in Electrical and Electronic Engineering, from the University of Peradeniya, Sri Lanka, in 2017. He earned his M.S. degree in Computer and Systems Engineering from Rensselaer Polytechnic Institute, New York, USA, in 2022. Currently, he is pursuing his Ph.D. degree in Robotics, Intelligent Systems, and Control at UC San Diego, California, USA. His research interests include control of infinite dimensional systems and event-triggered control.

Mamadou Diagne is an Associate Professor with the Department of Mechanical and Aerospace Engineering at the University of California San Diego, affiliated with the Department of Electrical and Computer Engineering. He completed his Ph.D. in 2013 at University Claude Bernard Lyon I, Villeurbanne (France). Between 2017 and 2022, he was an Assistant Professor with the Department of Mechanical Aerospace and Nuclear Engineering at Rensselaer Polytechnic Institute, Troy, New York. From 2013 to 2016, he was a Postdoctoral Scholar, first at the University of California San Diego, and then at the University of Michigan. His research focuses on the control of distributed parameter systems (DPS), adaptive control, time-delay systems, extremum seeking control and safe nonlinear control. He served as Associate Editor for Automatica, Systems & Control Letters and ASME Journal of Dynamic Systems, Measurement, and Control. He is Vice-Chair for Industry of the IFAC Technical Committee on Adaptive and Learning Systems and Vice-Chair for Education of the IFAC Technical Committee on Distributed Parameter Systems. He received the NSF Career Award in 2020.